Januario Da Costa Hossi*
Diakanua Nkazi
Josias van der Merwe
Atuman Samaila Joel
Kevin Graham Harding

# Desulfurization of Gasoline and Diesel by Fly Ash-Derived FAU Zeolite

Sulfur in fossil fuels is a major environmental and public health concern worldwide due to emissions of sulfur oxides formed during combustion. This may require new developments or upgrades of existing refining technologies. Hence, further desulfurization of gasoline and diesel to combat hazardous emissions could be a significant step toward environmental protection. In this study, adsorptive desulfurization of gasoline and diesel was achieved using a low-cost fly ash-derived faujasite (FAU) zeolite as complementary to the conventional hydrodesulfurization method. Sulfur levels of fuel samples, brought to the laboratory from typical fuel stations, were detected by a turbidimetric method before and after desulfurization. FAU zeolite sorbent, prepared from coal fly ash, was contacted with the fuel samples at stopped flow, and the residual fuels were analyzed to determine the sorbent's desulfurization performance. The process was optimized to enhance the sorbent's performance by varying the reaction conditions such as temperature, fuel volume, and the sorbent chemical composition. The results indicated that, at ambient temperature and pressure, the zeolitic desulfurization could reduce the sulfur content approximately by 40 % of its initial concentration, from 61 to 37 ppm and 155 to 97 ppm, in gasoline and diesel, respectively. Therefore, fly ash zeolites offer a possible opportunity for further desulfurization of refining petroleum fuels which may lead to economic and environmental gains.



**Keywords:** Adsorption, Desulfurization, Fuels, Zeolites

*Received:* April 13, 2023; *revised:* January 22, 2024; *accepted:* March 08, 2024

**DOI:** 10.1002/ceat.202300199

## 1 Introduction

Air emissions pose a serious threat to the environment and human health [1]. Besides being an air pollutant, sulfur has a blocking effect on many pollution control technologies affecting air emissions control [2]. Inadequate petroleum refining capacities have resulted in the importation of petroleum products around the world with nonuniform quality [3]; despite regulatory limits, petroleum fuels still contain significant levels of sulfur which causes the emission of sulfur oxides (SO*x*) that contribute to decreased air quality impacting adversely the environment and the human health [4, 5]. Every year, millions of metric tons of air pollutants are emitted worldwide into the atmosphere, and a significant part of these emissions come from the combustion of fossil fuels such as gasoline, diesel, and natural gas [1].

SO*x* are formed during the combustion of fossil fuels usually by internal combustion engines. As well as being environmentally detrimental, this substance is undesirable to the engine itself as it damages engine parts such as piston rings and cylinder [6, 7]. While countries' regulations for emissions reduction require extraordinary efforts to continue reducing sulfur levels in transportation fuels, particularly jet fuel, gasoline, and diesel [4], inadequate local petroleum refining capacities around the world have often resulted in the commercialization of petroleum products with nonuniform quality [3, 7]. Countries are rigorously continuing to reduce sulfur levels in automobiles, aviation, marine vessels, off-road vehicles, and other power-generating utilities limiting sulfur content in diesel and gasoline fuels to below 30 and 15 ppm, respectively [3, 8–10]. These restrictions may intensify the operating costs of the current hydrodesulfurization (HD) technology, which uses a Co-Mo/$Al_2O_3$ or Ni-Mo/$Al_2O_3$ catalyst at high temperatures and pressure, but is less effective in producing ultra-sulfur-free fuels [11, 12].

Dr. Januario Da Costa Hossi https://orcid.org/0000-0001-6663-6587 (januariodacosta.hossi@wits.ac.za), Prof. Diakanua Nkazi, Prof. Josias van der Merwe, Dr. Atuman Samaila Joel, Prof. Kevin Graham Harding
University of the Witwatersrand, School of Chemical and Metallurgical Engineering, 1 Jorissen St., Private Bag X3 Wits, 2050 Johannesburg, South Africa.

  

A promising technology that could complement HD for further and selective removal of sulfur compounds in petroleum fuels is adsorptive desulfurization (AD) by zeolite sorbent, which selectively removes sulfur compounds at ambient temperature and pressure without adsorbing aromatics and olefins present in the fuel [13–15]. Yang et al. [9] found that zeolite sorbents usually bond with sulfur adsorbates via a π-complexation mechanism. This uses electron charge donation from the *π-orbital* of the adsorbate to the vacant *s orbital* of the metal on zeolite, also known as *σ donation*. This is an important feature that renders the selectivity of thiophenes over benzene and olefins. Further studies by Yang et al. [9] revealed increased zeolitic adsorption capacity after cationic exchange of zeolite with transition metal cations such as potassium, silver, and copper could be performed by ionic exchange of starting zeolite with metal cations in liquid or solid. Thus, AD remains an exciting area to explore, and using coal fly ash (CFA) to prepare the zeolitic sorbent could turn desulfurization into an avenue for waste valorization and management.

This study assesses the merits of AD of petroleum fuels, namely, gasoline and diesel, using CFA-prepared faujasite (FAU) zeolite and optimizes the process by varying the reaction conditions such as temperature, contact time, and composition by cationic exchange of mother zeolite with appropriate transition metal cations to assess their effects on the desulfurization performance.

## 2 Materials and Method

### 2.1 Materials

Materials used for this study include substrates and chemical reagents such as CFA (Sasol Mining, Mpumalanga, South Africa); sodium hydroxide (NaOH); barium chloride ($Ba_2Cl$); metal salts such as potassium chloride (KCl), lithium chloride (LiCl), silver nitrate ($AgNO_3$), copper sulfate ($CuSO_4$), sodium chloride (NaCl), and anhydrous sodium sulfate ($Na_2SO_4$); gasoline and diesel fuels; glycerol ($C_3H_8O_3$); isopropyl alcohol ($C_3H_8O$); and hydrochloric acid (HCl).

### 2.2 Methods

#### 2.2.1 Preparation of FAU Zeolite

FAU zeolite was prepared from CFA via alkaline hydrothermal method [16–18]. The CFA was calcined at 850 °C for 2 h to remove volatile materials and unburned carbon, followed by acid treatment in 20 % HCl solution (10 mL HCl/g ash) to dealuminate and remove iron in CFA for the activation of aluminosilicate minerals [19]. The acid-treated CFA was then mixed with NaOH and fused in a stainless-steel tray at 550 °C for 2 h and cooled to room temperature. The sample was milled and dissolved with appropriate amounts of deionized water (10g CFA/100 mL) and aged for 6 h with stirring for colloidal formation at room temperature. The resulting gel was then transferred to a Teflon-lined stainless autoclave and kept undisturbed at 100 °C for 8 h for hydrothermal crystallization.

The synthesis was repeated with varying NaOH/CFA (wt./wt.) ratios (0.8–1.6), temperature (80–120 °C), and time (6–48 h) to determine the conditions that yielded the best zeolite structure. A portion of as-prepared FAU zeolite was ionically exchanged using appropriate alkaline ionic solutions of LiCl and $AgNO_3$ at mild temperatures (below 80°) for obtaining Li- and Ag-zeolite, respectively. The resulting solutions were cooled, washed with copious amounts of deionized water until a pH of approximately 9, filtered, and dried in an oven overnight at 100 °C. Mixed Li-Ag-zeolite was obtained by further exchanging Li-zeolite in $AgNO_3$.

#### 2.2.2 Determination of Sulfur Content by Turbidimetric Method

*Preparation of Reagents and Standard Series*

This study used a turbidimetric method [3] to determine sulfur content in liquid petroleum fuels. Gasoline (A) and diesel (B) fuel were collected from typical fuel stations and stored at room temperature for analysis and assessment. Each sample was treated with barium chloride for the formation of colloidal barium sulfate that absorbs light at a wavelength of around 400 nm. A conditioning reagent was prepared by mixing 50 $cm^3$ glycerol ($C_3H_8O_3$) with a solution containing 30 $cm^3$ concentrated hydrochloric acid (HCl), 300 $cm^3$ distilled water, 100 mL isopropyl alcohol ($C_3H_8O$), and 75 g sodium chloride (NaCl). Then, a blank solution was prepared of 100 mL distilled water and dispensed into a 250 mL Erlenmeyer flask, to which 5 $cm^3$ of previously prepared conditioning reagent was added and stirred for 5 min.

Twenty standard series of 20–400 ppm $SO_4^{2-}$ were prepared from anhydrous $Na_2SO_4$ dissolved with deionized water to desired concentrations of $SO_4^{2-}$. The correlation (unit conversion) below was used to determine the amount of $Na_2SO_4$ required to deliver 1g of $SO_4^{2-}$ as follows:

$$1\ \mathrm{g}\ SO_4^{2-}\left(\frac{1\ \mathrm{mol}\ SO_4^{2-}}{96.06\ \mathrm{g}\ SO_4^{2-}}\right)\left(\frac{1\ \mathrm{mol}\ Na_2SO_4}{1\ \mathrm{mol}\ SO_4^{2-}}\right)\cdot\left(\frac{142.04\ \mathrm{g}\ Na_2SO_4}{1\ \mathrm{mol}\ Na_2SO_4}\right) \quad (1)$$

Exactly 1 g (1000 mg) $SO_4^{2-}$ was dissolved in a liter of distilled water to prepare a solution of 1000 ppm $SO_4^{2-}$. Standard dilution series from 20 to 400 ppm $SO_4^{2-}$, in increments of 20 ppm, were prepared using the dilution equation (Eq. (2)) as summarized in Tab. 1. These concentrations gave the calibration plot which was used to determine the sulfur concentration of unknown samples.

$$\text{Concentration initial} \times \text{Volume initial} = \text{Concentration final} \times \text{Volume final} \quad (2)$$

*Absorbance Measurement of Standard Series and Blank*

The absorbance was measured by ultraviolet–visible (UV/vis) spectroscopy (Shimadzu UV-1800 Spectrophotometer). The absorbance of the blank was measured first; the blank solution was stirred, and while stirring, a spoonful of $BaCl_2$ crystal was dissolved in 2 mL distilled water and added to the solution, and the

  

**Table 1.** Standard dilution series.

| Series | $C_1$ [ppm] | $V_1$ [mL] | $C_2$ [ppm] | $V_2$ [mL] | Series | $C_1$ [ppm] | $V_1$ [mL] | $C_2$ [ppm] | $V_2$ [mL] |
|---|---|---|---|---|---|---|---|---|---|
| 1 | 1000 | 50 | 20 | 2500 | 11 | 1000 | 50 | 220 | 227 |
| 2 | 1000 | 50 | 40 | 1250 | 12 | 1000 | 50 | 240 | 208 |
| 3 | 1000 | 50 | 60 | 833 | 13 | 1000 | 50 | 260 | 192 |
| 4 | 1000 | 50 | 80 | 625 | 14 | 1000 | 50 | 280 | 179 |
| 5 | 1000 | 50 | 100 | 500 | 15 | 1000 | 50 | 300 | 167 |
| 6 | 1000 | 50 | 120 | 417 | 16 | 1000 | 50 | 320 | 156 |
| 7 | 1000 | 50 | 140 | 357 | 17 | 1000 | 50 | 340 | 147 |
| 8 | 1000 | 50 | 160 | 313 | 18 | 1000 | 50 | 360 | 139 |
| 9 | 1000 | 50 | 180 | 278 | 19 | 1000 | 50 | 380 | 132 |
| 10 | 1000 | 50 | 200 | 250 | 20 | 1000 | 50 | 400 | 125 |

The letters $C_1$, $C_2$, $V_1$, and $V_2$ are the initial and final concentrations [ppm] and volumes [mL] of the standard series.

stirring was stopped. A portion of this solution was poured into a cuvette, and the spectra of the blank were measured at a wavelength range of 260–740 nm. Then, each of the increments was measured at the same wavelength range, and the wavelength that gave maximum absorbance was fixed and considered for plotting the calibration curve.

Finally, the sulfur content was measured in fuels; 100 $cm^3$ of each sample A and B was dispensed into a 250 mL Erlenmeyer flask to which 5 $cm^3$ conditioning reagent was added and stirred for 5 min. A spoonful of $BaCl_2$ was dissolved in 2 $cm^3$ of distilled water and was added to the solution. Some of the solution was poured into a cuvette, and the absorbance was read immediately at the fixed wavelength.

*Determination of Sulfur Content*

Lambert–Beer's Law [15] was applied for the determination of unknown concentration of sulfur in gasoline and diesel. The equation of line Eq. (3), from the calibration curve, and the relation in Eq. (4) were used to determine the concentration of $SO_4^{2-}$ which led to the quantification of sulfur in the fuel.

$$Y = mx + c \tag{3}$$

$$\frac{\text{mg } SO_4^{2-}\left(\frac{1 \text{ mmol } SO_4^{2-}}{96.06 \text{ mg } SO_4^{2-}}\right)\left(\frac{1 \text{ mmol S}}{1 \text{ mmol } SO_4^{2-}}\right)\left(\frac{32 \text{ mg S}}{1 \text{ mmol S}}\right)}{\text{L}} = \text{S}\left(\frac{\text{mg}}{\text{L}}\right) \tag{4}$$

### 2.2.3 Adsorptive Desulfurization Procedure

AD of refined petroleum fuels, namely, gasoline and diesel, was achieved by contacting the fuels with fly ash-derived FAU zeolite at batch conditions (Fig. 1).

Gasoline or diesel fuels (10 mL) were held inside a vessel to which a zeolite (1 g) was added. The reaction was kept undisturbed for an hour. After that, some fuel was removed from the solution and analyzed to determine the residual sulfur concentration (see Sect. 2.2.2). The influence of temperature and

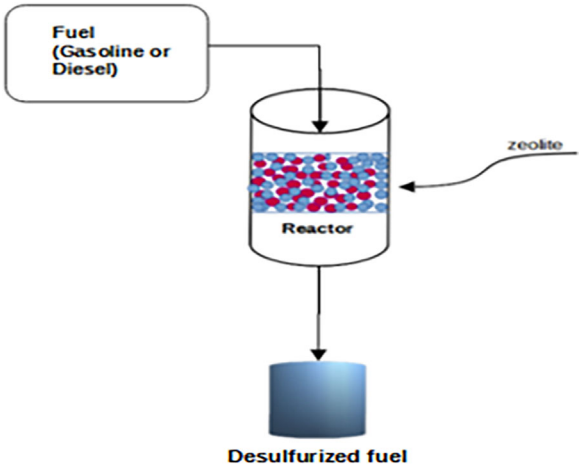


**Figure 1.** Flow diagram of desulfurization of gasoline and diesel by FAU zeolite.

adsorbent's chemical composition on desulfurization performance was evaluated by varying the desulfurizing temperature (25–100 °C), zeolite Si:Al ratio (1, 2, and 3), and cationic exchanging the starting zeolite with $Cu^+$, $Ag^+$, and $K^+$. To modify the Si:Al ratio, the starting zeolite material was contacted with a known amount of silica ($Na_2SiO_3$) or alumina source ($Al_2(SO_4)_3$), depending on whether more silicon or aluminum was required, in alkaline conditions with mild heating, followed by washing, filtration, and drying [13, 14]. The cationic exchange was achieved by contacting the starting zeolite with an appropriate amount of aqueous $AgNO_3$, $CuSO_4$, and KCl to source $Ag^+$, $Cu^{2+}$, and $K^+$ cations, respectively. Each exchange solution was heated to 80 °C for 5 min and immediately washed with deionized water, filtrated, and dried to recover the crystals.

Sulfur uptake by the adsorbent and desulfurization capacity was calculated by taking the difference in the mass of sulfur in the fuel before and after desulfurization per gram of adsorbent Eq. (5).

$$\text{Desulfurization capacity}\left(\frac{\text{mg}}{\text{g}}\right) = \frac{\text{sulfur concentration (ppm)} \times \text{fuel Volume (L)}}{\text{Mass of adsorbent (g)}} \tag{5}$$

## 2.3 Analysis and Characterization

Scanning electron microscopy (SEM) and energy-dispersive X-ray spectroscopy (EDS) were used to determine the morphology and elemental composition of the as-prepared zeolite, respectively. $N_2$-adsorption, by Brunauer–Emmett–Teller (BET) method, was used to measure surface area, pore size, and pore volume distribution of the crystal, Fourier-transform infrared (FTIR) was used to analyze chemical groups present in the as-prepared zeolite, and UV/vis spectroscopy was used to measure the absorbance of gasoline and diesel fuels before and after AD for the determination of sulfur content.

  

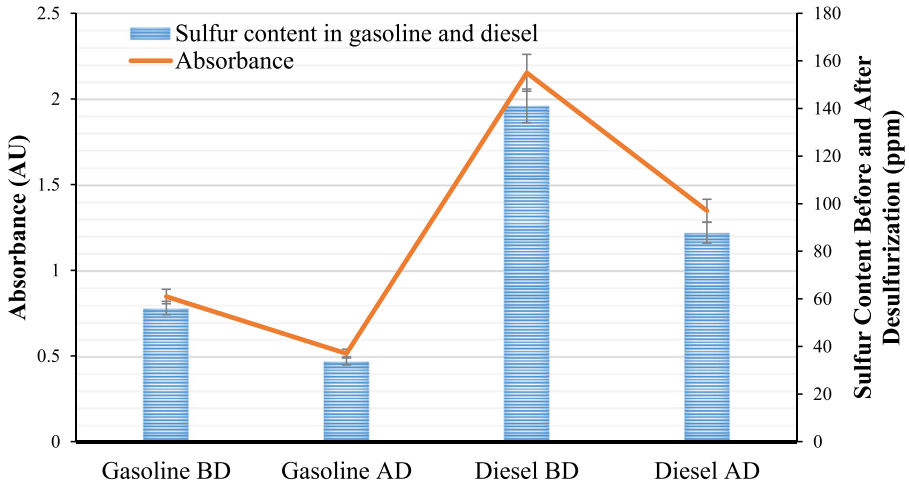


**Figure 2.** Sulfur uptake by zeolitic adsorptive desulfurization.

## 3 Results

### 3.1 Desulfurization Assessment

An analysis by UV/vis spectroscopy revealed a sulfur concentration of 155 and 91 ppm, with an absorbance of 0.78 and 1.98 (AU), for gasoline and diesel, respectively. These values are still high to the current requirements limiting sulfur content to 10 ppm in fuels [18]. The removal of sulfur in refined petroleum fuels was achieved by AD using FAU zeolite (Fig. 2).

The correlation of the absorbance of known sulfur concentrations of standard series with the sulfur content of gasoline and diesel can be found in the supplementary data (Appendix); BD and AD, depicting the blue bars in Fig. 2, are the sulfur concentrations before desulfurization and after desulfurization, respectively. The content of sulfur dropped approximately by 40 % of its initial concentration, from 155 to 97 ppm in diesel and from 61 to 37 ppm in gasoline, which is a satisfactory decrease that may positively influence the reduction of SO*x* emission. This was achieved at ambient pressure and room temperature which could make zeolitic AD promising and economically attractive for the refiners.

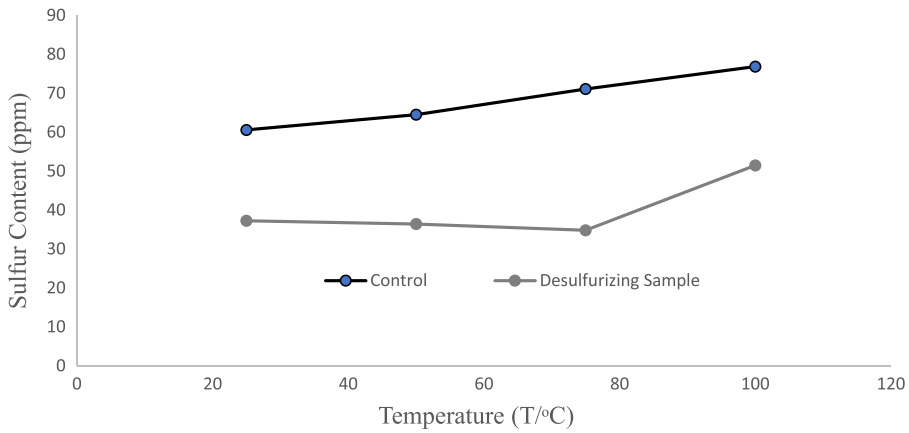


**Figure 3.** Temperature effects on desulfurization performance.

#### 3.1.1 Influence of Temperature on Desulfurization Performance

The influence of temperature on AD is depicted in Fig. 3. The temperature was varied from 25 °C to 100 °C, and a control sample, subjected to the same desulfurizing conditions, without zeolite in it, was used to monitor the change of the desulfurizing fuel.

As observed in Fig. 3, heating the reaction solution moderately improved the desulfurization performance. However, a rise in the concentration of residual fuel was registered at temperatures above 70 °C. This could be due to the volatilization of lighter hydrocarbons, like olefins and aromatics, leaving other components in fuel, such as sulfur, more concentrated, or perhaps some kinetic and thermodynamic effects kicking in due to the rise in temperature. This indicates that AD of fuels is suitable, at relatively lower temperatures, below 80 °C.

#### 3.1.2 Influence of Si:Al Ratio on Desulfurization Performance

Zeolite properties depend largely on their structure and Si:Al ratio which can be adjusted to suit different applications [15]. Increasing the Si:Al ratio from 1.4 to 2 improved sulfur uptake by zeolite sorbent (mg sulfur/g sorbent) from 0.24 to 0.32 mg $g^{-1}$ (Fig. 4).

Increasing the Si:Al ratio substantially advanced the zeolitic desulfurization performance by doubling the adsorption capacity from approximately 0.20 mg $g^{-1}$ at Si:Al ratio of 1.5 to 0.40 mg $g^{-1}$ at Si:Al of 2.5. Nevertheless, the adsorption capacity dropped to <0.15 mg $g^{-1}$ from 0.40 mg $g^{-1}$ when the Si:Al ratio was increased beyond 2.5 (Fig. 4). This indicates that Si:Al ratios between 1 and 2.5 offer the best zeolitic AD performance. Evidence to justify this tendency could be the low aluminum content that lowers the Lewis acidity and the number of aluminum complexation sites associated with the zeolite which affects the adsorption of sulfur when more silicon is introduced in zeolite [19, 20].

#### 3.1.3 Influence of Cationic Exchange on Desulfurization Performance

The AD capacity trend of different cationic-exchanged zeolites is displayed in Fig. 5: FAU-zeolite > K-zeolite > Cu-zeolite > Ag-zeolite.

It is apparent from the desulfurization performance of different

  

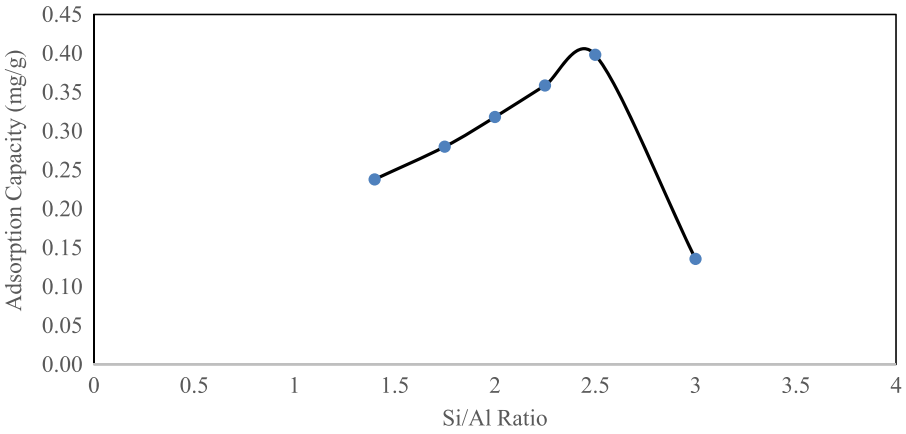


**Figure 4.** Effects of Si:Al ratio on desulfurization performance.

ionic-exchanged zeolites in Fig. 5 that the starting FAU zeolite and K-zeolite demonstrated better desulfurization capacity (0.9 mg $g^{-1}$) than the other cationic-exchanged zeolites. K-zeolite showed near or the same desulfurization capacity as the starting FAU zeolite followed by Ag-zeolite at 5 mg $g^{-1}$. Cu-zeolite was the lowest desulfurizing sorbent at around 1.2 mg $g^{-1}$ desulfurization capacity. Cu-exchanged zeolite has a reasonably greater desulfurization capacity than Ag-zeolite. According to Lee and Valla [19], the coexistence of reduced $Cu^{+}$ (having electronic configuration of $1S^2 2S^2 2p^6 3S^2 3d^{10} 4S^0$) with $Cu^{2+}$ form leaves a vacant s-orbital desirable for $\pi$-complexation which is beneficial to AD. Thus, Cu-zeolite was expected to perform relatively better. It is not yet understood why cationic-exchanged zeolites did not improve the desulfurization performance, although Lee and Valla [19] and Gong et al. [21] believed that cationic exchange could improve the AD performance. The desulfurization performance of Ag-zeolite was very poor. Evidence shows that hydrated silver compounds are light sensitive [19, 20], the reason why, commonly, reactions involving silver-containing substances are conducted in dark environments. Possibly, performing the process of desulfurization under normal ambient conditions did not create an adequate environment when silver-containing zeolite was used as a sorbent.

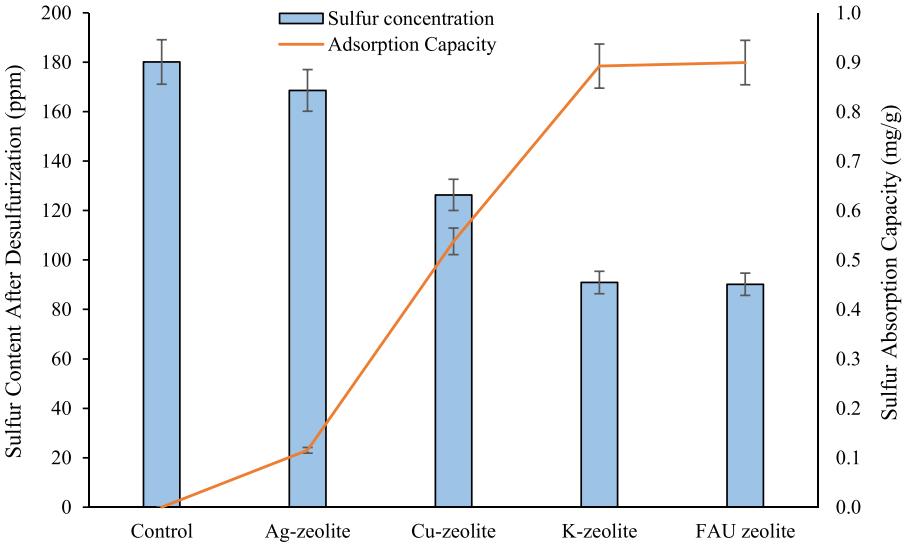


**Figure 5.** Effects of cationic exchange on desulfurization performance.

## 3.2 Adsorbent Characterization

### 3.2.1 X-Ray Diffraction Analysis

It is quite uneasy to compare FAU zeolite-Y with its zeolite-X analogous using X-ray diffraction (XRD) [21–24]. However, these structures are of the same low silica FAU family that are only differentiated by their Si:Al ratios (1–1.5 for zeolite-X and 1.5–3 for zeolite-Y) [24].

The XRD of the as-synthesized FAU zeolite (Fig. 6) shows a series of peaks at the theta region characteristic of a low silica zeolite [25, 26]. Further evidence was given by the EDS which revealed a Si:Al ratio of 1.4 confirming the success of the synthesis of FAU zeolite-X.

### 3.2.2 SEM and EDS Analysis

SEM-EDS was used to analyze the morphology and elemental composition of untreated and treated CFA. EDS analysis revealed the as-received CFA comprising 21 wt. % Si, 56 wt. % $O_2$, and 16.5 wt. % $Al_2$, which confirmed its suitability for zeolite production given the satisfactory amount of silica and alumina contained. Raw CFA contained trace mineral elements such as potassium, calcium, titanium, and iron which were absent in the treated CFA. Treated CFA revealed Si:Al ratios ranging from 1.4 to below 1.6 which falls under the law of silica FAU-type zeolite family [24].

Fig. 7(a and b) illustrates backscattered electron images of untreated and treated CFA acquired at 20 kV.

The typical morphology of raw CFA presents abundant spheres associated with coarser and anhedral porous lumps of material illustrated in Fig. 7(a). In Fig. 7(b), fine angular particles are visible indicating that zeolite formation has been achieved. These angular particles were mostly obtained in fly ash treated at a NaOH/Ash ratio of 1.6 resulting in the formation of euhedral (well-formed crystal) aggregates of zeolite crystals.

### 3.2.3 BET Analysis

Physical properties of zeolites, such as specific surface area, pore size, and

  

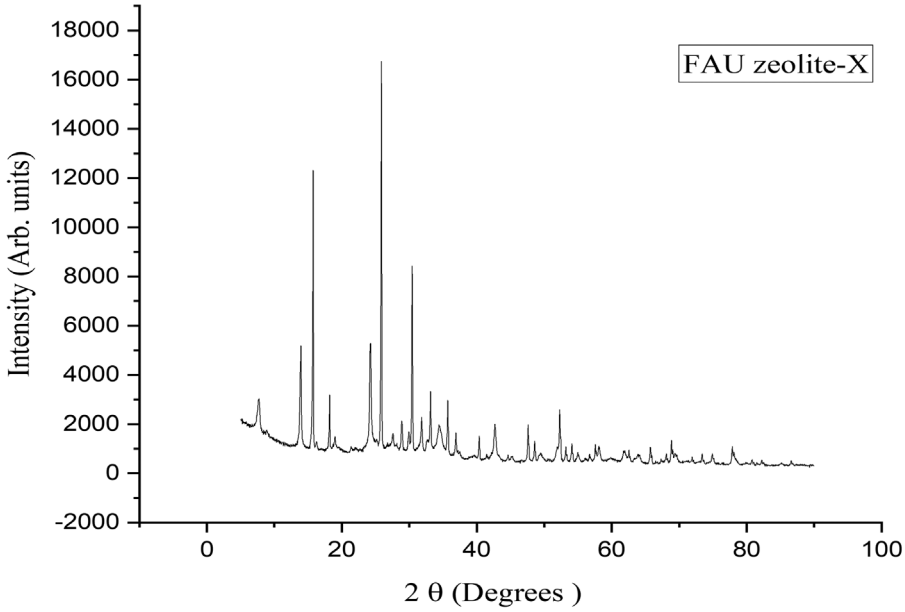


**Figure 6.** XRD patterns of the as-synthesized FAU zeolite.

**Table 2.** Surface area and pore structure of FAU zeolite analysis by BET.

| Sample | BET [$m^2\ g^{-1}$] | Pore width [nm] | Pore vol. [$cm^3\ g^{-1}$] | Particle size [nm] |
|---|---|---|---|---|
| FAU zeolite | 60.54 | 1.04 | 0.07 | 99.73 |

pore volume distribution, are important factors in various zeolite applications. BET measurements of the as-prepared FAU zeolite are presented in Tab. 2.

BET surface area of FAU zeolite is relatively large (60 $m^2g^{-1}$) which is desirable for adsorption. According to Murphy [25], large surface areas are beneficial for adsorption as these increase the sorbent loading capacity. However, exclusion by molecular size (sieving) is not the only separation parameter considered in adsorptive separation; the Lewis acidity of zeolite, due to its central metal cation, plays a great part in the adsorption of chemical species rendering electrostatic interactions between the adsorbent and the adsorbate [25, 27].

### 3.2.4 Fourier-Transform Infrared Spectroscopy

The functional groups and molecular bonding of as-produced FAU zeolite were analyzed by FTIR spectroscopy as illustrated in Fig. 8.

FTIR spectrum revealed no organic chemical groups. This indicates the absence of contamination with organic chemical species of the synthesized FAU zeolite crystals. The weak peaks that appear over 3376.24 $cm^{-1}$ and 1638 $cm^{-1}$ are characteristic of O–H stretching and bending due to structural and nonstructural adsorbed water molecules; only the most intense peak (9670 $cm^{-1}$) corresponds to vibrations due to tetrahedral asymmetric linkages. The remaining peaks at 674 $cm^{-1}$ and below indicate the presence of ring linkages in zeolite structure [22].

## 4 Conclusions

SO*x* emissions from refined petroleum fuels reduce air quality. Despite regulation restrictions, refined petroleum products have high sulfur levels that exceed environmental standards. HD techniques may not produce ultra-low sulfur fuels or could be too expensive to achieve the target level. Thus, adding HD to AD may avoid possible refining costs and improve efficiency. In diesel and gasoline, zeolitic AD reduced sulfur from 155 to 100 ppm and 61 to 37 ppm at stopped-flow and ambient conditions. This study found that the Si:Al ratio of 2 performed best for zeolitic desulfurization. The desulfurization capability of unmodified FAU zeolite was much higher than that of Cu- and Ag-zeolites, except for K-zeolite, which performed reasonably. Thus, desulfurization with unmodified FAU zeolite may suffice. In most coal-energy-dependent countries, CFA is a plentiful waste. Using it to make zeolite materials may have environmental benefits and allow waste valorization. Thus,

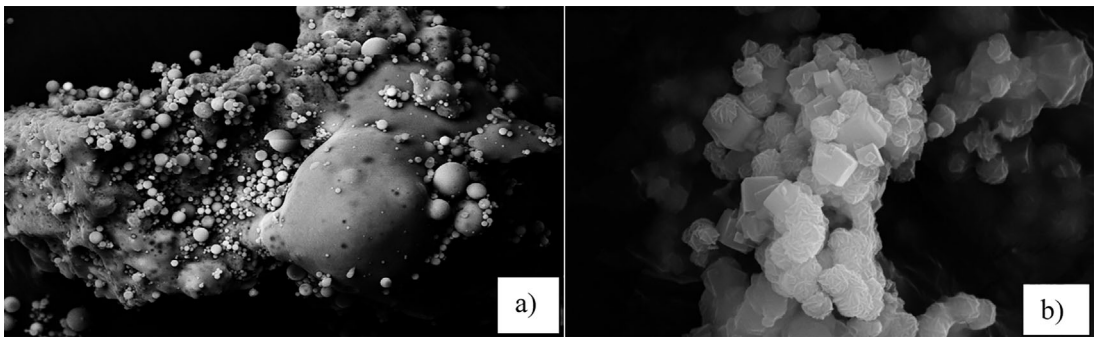


**Figure 7.** Backscattered electron images of (a) raw coal fly ash and (b) as-prepared FAU zeolite.

  

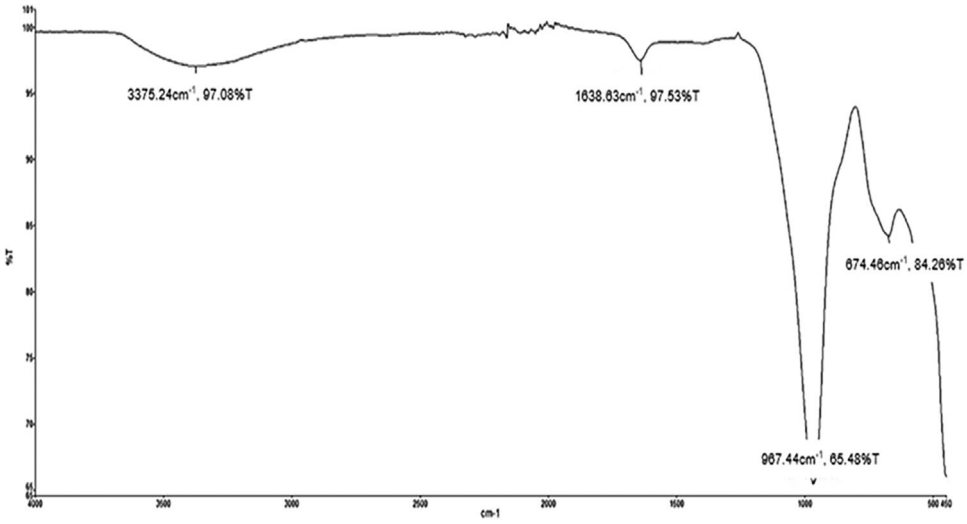


**Figure 8.** FTIR spectrum of the as-synthesized FAU zeolite.

zeolitic desulfurization of petroleum fuels could become a well-established energy technology that complements HD techniques and improves the environmental performance of fossil fuels.

## Acknowledgment

The authors would like to acknowledge the financial support from the University Research Council of the University of Witwatersrand, Johannesburg, and declare that there is no conflict of interests, affiliations, or involvement of entity with any the financial or non-financial interest in the subject matter or materials discussed in this manuscript.

## Appendix

### UV/vis analysis

The absorbance by ultraviolet–visible (UV/vis) spectroscopy of known sulfur concentrations of standard series (20 to 400 ppm), prepared in the laboratory (Tab. 1), was correlated to the absorbance of gasoline and diesel to determine the sulfur concentration of desulfurizing fuels. Fig. A1 shows the absorption spectrum of the standard dilution series.

The UV/vis measurements at 407.5 nm gave the maximum absorbances that were used for plotting the calibration curve (Fig. A2).

Absorbances for gasoline and diesel were 0.78 and 1.98 (AU), respectively, before adsorptive desulfurization. A straight line equation of the calibration curve (Fig. A2) and Eqs. (3) and (4) were used to correlate the unknown concentration of sulfur in gasoline and diesel with the known concentrations of the standards. Based on these correlations, the concentration of sulfur was found to be 61 ppm in gasoline and 155 ppm in diesel before adsorptive desulfurization. These values are still high to the current requirements limiting sulfur content to 10 ppm in fuels [18].

## Abbreviations

| | |
|---|---|
| AD | adsorptive desulfurization |
| BET | Brunauer–Emmett–Teller |
| EDS | energy-dispersive X-ray spectroscopy |

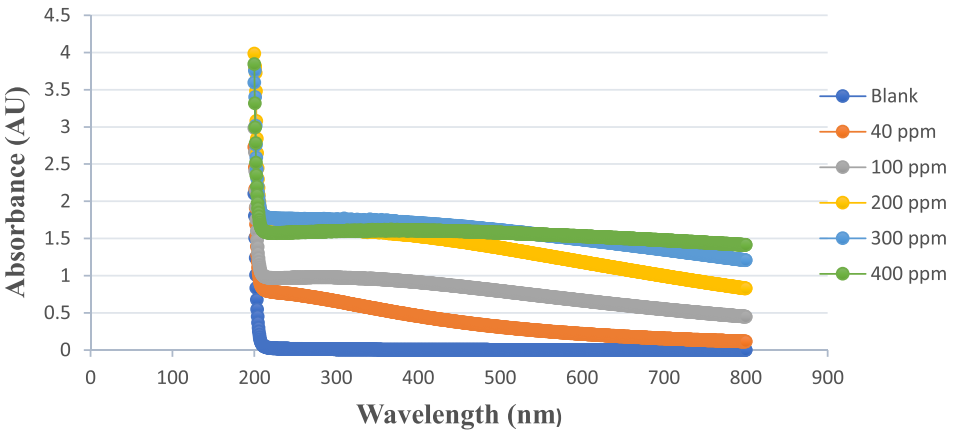


**Figure A1.** Absorption spectra of standards.

  

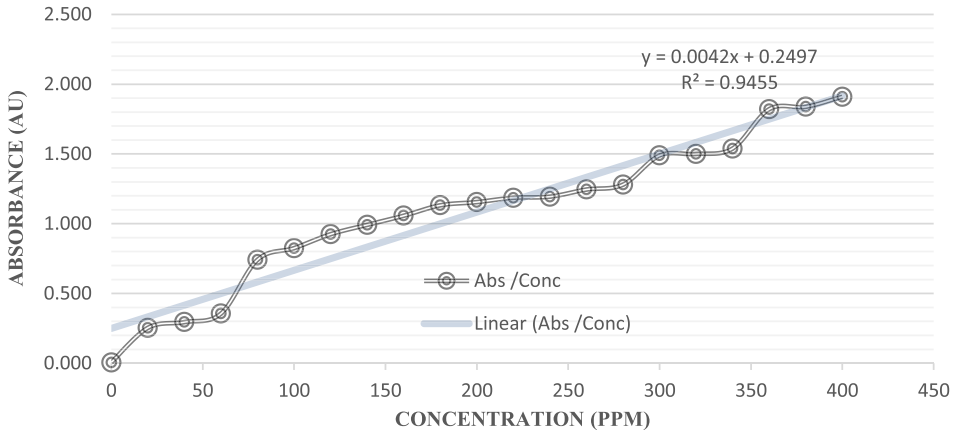


**Figure A2.** Linear fit of plot of absorbance versus concentration of standards.

| | |
|---|---|
| CFA | coal fly ash |
| FAU | ash-derived faujasite |
| FTIR | Fourier-transform infrared |
| HD | hydrodesulfurization |
| SEM | scanning electron microscopy |
| UV/vis | ultraviolet–visible |
| XRD | X-ray diffraction |

## References


[1] L. M. Guerrero, J. F. Mendoza, K. T. V. Ong, E. M. Olegario-Sanchez, E. L. Ferrer, *Arab. J. Sci. Eng.* **2019**, *44* (*6*), 5581–5588. DOI: https://doi.org/10.1002/10.1007/s13369-019-03882-y

[2] K. W. Blumberg, M. P Walsh, C. Pera, Meeting of the International Council on Clean Transportation, Napa CA, May **2003**. https://theicct.org/sites/default/files/publications/Low-Sulfur_ICCT_2003.pdf (Accessed on January 05, 2024)

[3] O. S. Olatunji, L. A. Jimoda, B. S. Fakinle, J. A. Adeniran, J. A. Sonibare, *Pet. Sci. Technol.* **2015**, *33* (*1*), 102–109. DOI: https://doi.org/10.1002/10.1080/10916466.2014.920028

[4] S. Velu, C. Song, M. H. Engelhard, Y. H. Chin, *Ind. Eng. Chem. Res.* **2005**, *44* (*15*), 5740–5749. DOI: https://doi.org/10.1002/10.1021/ie0488492

[5] J. A. Sonibare, L. A. Jimoda, *Part A: Recover Util. Environ. Eff.* **2009**, *31* (*11*), 923–935. DOI: https://doi.org/10.1002/10.1080/15567030801904517

[6] R. Alam, J. Q. Shang, X. Cheng, *Environ. Monit. Assess.* **2012**, *184* (*5*), 3373–3387. DOI: https://doi.org/10.1002/10.1007/s10661-011-2195-3

[7] C. Ngamcharussrivichai, C. Chatratananon, S. Nuntang, P. Prasassarakich, *Fuel* **2008**, *87* (*10–11*), 2347–2351. DOI: https://doi.org/10.1002/10.1016/j.fuel.2007.10.003

[8] M. Xue, R. Chitrakar, K. Sakane, T. Hirotsu, K. Ooi, Y. Yoshimura, *J. Colloid Interface Sci.* **2006**, *298* (*2*), 535–542. DOI: https://doi.org/10.1002/10.1016/j.jcis.2005.12.051

[9] R. T. Yang, A. J. Hernández-Maldonado, F. H. Yang, *Science* **2003**, *301* (*5629*), 79–81 DOI: https://doi.org/10.1002/10.1126/science.1085088

[10] K. Ojha, N. C. Pradhan, A. N. Samanta, *Bull. Mater. Sci.* **2004**, *27* (*6*), 555–564. DOI: https://doi.org/10.1002/10.1007/BF02707285

[11] C. Wang, J. Li, X. Sun, L. Wang, X. Sun, *J. Environ. Sci.* **2009**, *21* (*1*), 127–136. DOI: https://doi.org/10.1002/10.1016/S1001-0742(09)60022-X

[12] L. Ayele, J. Pérez-Pariente, Y. Chebude, I. Díaz, *Appl. Clay Sci.* **2016**, *132–133*, 485–490. DOI: https://doi.org/10.1002/10.1016/j.clay.2016.07.019

[13] O. Eterigho-ikelegbe, S. Bada, M. O. Daramola, R. Falcon, *Mater. Today Proc.* **2021**, *7* (*38*), 675–681. DOI: https://doi.org/10.1002/10.1016/j.matpr.2020.03.693

[14] H. Liu, *ACS Omega* **2022**, *7* (*23*), 20347–20356. DOI: https://doi.org/10.1002/10.1021/acsomega.2c02388

[15] W. Mäntele, E. Deniz, *Spectrochim. Acta Part A: Mol. Biomol. Spectrosc.* **2017**, *173*, 965–968. DOI: https://doi.org/10.1002/10.1016/j.saa.2016.09.037

[16] N. Shigemoto, H. Hayashi, K. Miyaura, *J. Mater. Sci.* **1993**, *28* (*17*), 4781–4786. DOI: https://doi.org/10.1002/10.1007/BF00414272

[17] A. Ates, *Powder Technol.* **2019**, *344*, 199–207. DOI: https://doi.org/10.1002/10.1016/j.powtec.2018.12.018

[18] Y. Xie, F. Posada, R. Minjares, *Diesel sulfur content impacts on Euro VI soot-free vehicles: Considerations for emerging markets*, Working Paper 2020-11, International Council on Clean Transportation, Wilmington, DE **2020**. https://theicct.org/wp-content/uploads/2021/06/50ppm-diesel-sulfur-05222020.pdf (Accessed on December 08, 2023)

[19] K. X. Lee, J. A. Valla, *React. Chem. Eng.* **2019**, *4* (*8*), 1357–1386. DOI: https://doi.org/10.1002/10.1039/C9RE00036D

[20] P. W. Du Plessis, T. V. Ojumu, O. O. Fatoba, R. O. Akinyeye, L. F. Petrik, *Mater.* **2014**, *7* (*4*), 3305–3318. DOI: https://doi.org/10.1002/10.3390/ma7043305

[21] Y. Gong, T. Dou, S. Kang, Q. Li, Y. Hu, *Fuel Process. Technol.* **2009**, *90* (*1*), 122–129. DOI: https://doi.org/10.1002/10.1016/j.fuproc.2008.08.003

[22] N. D. Hutson, R. T. Yang, *AIChE J.* **2000**, *46* (*11*), 2305–2317. DOI: https://doi.org/10.1002/10.1002/aic.690461121

[23] F. E. Epiepang, X. Yang, J. Li, Y. Wei, Y. Liu, R. T. Yang, *Chem. Eng. Sci.* **2018**, *198*, 43–51. DOI: https://doi.org/10.1002/10.1016/j.ces.2018.12.048

[24] M. Lassinantti, *Synthesis, Characterization and Properties of Zeolite Films and Membranes*, BEng Thesis, Lulea University of Technology **2001**.

[25] K. Murphy, *Are Nitrogen Molecules Really Larger Than Oxygen Molecules? The correct answer, with respect to "permeation", is*


  

*yes*., https://www.getnitrogen.org/pdf/graham.pdf (Accessed on November 17, 2023)
[26] M. M. J. Treacy, J. B. Higgins, *Collection of Simulated XRD Powder Patterns for Zeolites*, 5th ed., Elsevier **2007**.
[27] J. D. C. Hossi, D. Nkazi, J. van der Merwe, K. Harding, *In Int. Conf. on Sustainable Engineering and Materials Development* (Eds: A. A. Abioye, O. O. Ajayi, B. J. Babalola, O. Adesina, O. E. Bamidele) **2023**.

  